Molecular Crystals and Liquid Crystals

Publication details, including instructions for authors and subscription information:
http://www.tandfonline.com/loi/gmcl20

Proton Presence and Motion in Rhenium-Oxide Films and Their Application to Liquid-Crystalline Cells

M. Castriota [a], E. Cazzanelli [a], G. Das [b], R. Kalendarev [c], A. Kuzmin [c], S. Marino [a], G. Mariotto [b], J. Purans [c b] & N. Scaramuzza [a]

[a] ISTITUTO Nazionale per la Fisica Della Materia-liquid Crystal Laboratories and Centro Di Eccellenza Materiali innovativi Funzionali Calabria, Department of Physics, University of Calabria, Rende, Italy

[b] Physics Department, University of Trento, Povo, Italy

[c] Institute of Solid State Physics, University of Latvia, Riga, Latvia

Version of record first published: 22 Sep 2010

To cite this article: M. Castriota, E. Cazzanelli, G. Das, R. Kalendarev, A. Kuzmin, S. Marino, G. Mariotto, J. Purans & N. Scaramuzza (2007): Proton Presence and Motion in Rhenium-Oxide Films and Their Application to Liquid-Crystalline Cells, Molecular Crystals and Liquid Crystals, 474:1, 1-15

To link to this article: http://dx.doi.org/10.1080/15421400701693435

Mol. Cryst. Liq. Cryst., Vol. 474, pp. 1–15, 2007

ISSN: 1542-1406 print/1563-5287 online
DOI: 10.1080/15421400701693435

Proton Presence and Motion in Rhenium-Oxide Films and Their Application to Liquid-Crystalline Cells

M. Castriota
E. Cazzanelli
ISTITUTO Nazionale per la Fisica Della Materia-liquid Crystal Laboratories and Centro Di Eccellenza Materiali innovativi Funzionali Calabria, Department of Physics, University of Calabria, Rende, Italy

G. Das
Physics Department, University of Trento, Povo, Italy

R. Kalendarev
A. Kuzmin
Institute of Solid State Physics, University of Latvia, Riga, Latvia

S. Marino
ISTITUTO Nazlonale per la Fisica Della Materia-liquid Crystal Laboratories Laboratory and Centro Di Eccellenza Materiali innovativi Funzlonali Calabria, Department of Physics, University of Calabria, Rende, Italy

G. Mariotto
Physics Department, University of Trento, Povo, Italy

J. Purans
Institute of Solid State Physics, University of Latvia, Riga, Latvia; Physics Department, University of Trento, Povo, Italy

N. Scaramuzza
ISTITUTO Nazlonale per la Fisica Della Materia-liquid Crystal Laboratories Laboratory and Centro Di Eccellenza Materiali innovativi Funzlonali Calabria, Department of Physics, University of Calabria, Rende, Italy

Address correspondence to N. Scaramuzza, ISTITUTO Nazlonale per la Fisica Della Materia-liquid Crystal Laboratories Laboratory and Centro Di Eccellenza Materiali innovativi Funzlonali Calabria, Department of Physics, University of Calabria, Ponte P. Bucci Cubo 31C, I-87036 Rende, CS, Italy. E-mail: scaramuzza@fis.unical.it

Disordered solid phases, containing appreciable amounts of hydrogen ions, are grown at the surface of rhenium oxide crystals, because of the high reactivity of this compound with ambient moisture. To investigate such phenomena, a comparative study is performed on ground powder and thermally evaporated or sputtered films using x-ray diffraction and micro-Raman spectroscopy. Two types of solid phases were found in the films: H_xReO_3 distorted perovskite structures, based on corner-sharing ReO_6 octahedra as in the bulk crystals, and ordered $HReO_4$ crystalline structures, based on tetrahedral perrhenate ions. The complex impedance measurements on ReO_3 films support the hypothesis of mobile hydrogen ions in such defective films. Moreover, this relevant protonic conductivity allows the application of these films as active layers inserted into asymmetric nematic liquid-crystalline cells to rectify the electro-optical response of such devices, with performances quite similar to previously studied oxides such as WO_3.

INTRODUCTION

Because of its conductivity properties, rhenium oxide can be very useful for technological applications, such as SOFCs (solid oxide fuel cells), electrochromic devices, solid-state batteries, and other particular applications.

Rhenium trioxide appears red colored and shows metallic conductivity at temperatures less than 500 K [1–4]. The bulk rhenium-trioxide crystal belongs to the space group $O^1{}_h(Pm3\,m)$ with the lattice parameter $a_0 = 3.7504$ Å [5]. Its crystal lattice is composed of ReO_6 octahedra joined by corners, and the Bravais unit cell contains one unit of ReO_3. The cubic lattice of ReO_3 is very stable at normal pressure for all the temperatures [5,6]. The $Re^{6+}(5d^1)$ configuration with one d-electron in the conduction band, in excess with respect to tungsten trioxide, justifies the high electronic conductivity, similar to the one of tungsten bronze [7].

A recent work [8] on Raman spectroscopy and vibrational dynamics of ReO_3 indicates that a different kind of disorder is always present at the surface of powders and thin films of ReO_3. Both electronic and ionic conductivities can be observed in actual samples of rhenium trioxide, with the ionic one associated to intercalated hydrogen cations coming from the moisture reaction with a subsurface layer of the oxide:

$$(1+x)\mathrm{Re}O_3 + xH_2O \rightleftarrows H_x\mathrm{Re}O_3 + xH\mathrm{Re}O_4.$$

The defective system of H_xReO_3 and $HReO_4$, formed in this reaction, is described as an amorphous layer [9]. The hydrogen concentration in commercial ReO_3 powders is higher in the layers closer to the surface, and when the temperature is greater than 200°C, the intercalated protons leave the host oxide and a sublimation occurs for the ReO_3 layers

closer to the surface [9], which can be exploited to grow thin films on various substrates.

This work is aimed at investigating some of the properties of the disordered solid phases of ReO_3 different from bulk crystals, which can be more promising for the potential applications: fine-grained powders obtained by grinding and rhenium-oxide thin film obtained by thermal evaporation and magnetron reactive sputtering on various substrates. X-ray diffraction (XRD) and micro-Raman spectroscopy have been exploited for the study of the basic structural properties of these samples.

Preliminary measurements on the ionic (protonic) conductivity of these films have been performed, and a specific application using the ionic conductivity has been investigated as was done for other metal-oxide films [10–16]: the ability of such oxide to rectify the electro-optical response of the asymmetric nematic liquid-crystalline cells has been measured by inserting rhenium-oxide thin films deposited on ITO (indium-doped tin oxide)–coated glasses as asymmetric electrodes in such cells.

EXPERIMENTAL

Rhenium oxide (99.9% purity) was supplied by Metalli Preziosi SpA as polycrystalline powder. Some amounts of the powder underwent milling processes of variable time duration up to 10 min, manually performed in an agate mortar. Thin films were obtained by simple evaporation of the powders when the temperature reached the range 200–250°C; in fact, above 200°C, a strong sublimation occurs in rhenium oxide. For the evaporation on glasses and on ITO-coated glasses used for electro-optical test in liquid-crystalline cells, the powder and the substrate have been maintained inside a big oven, at constant temperature of 210°C for typical durations of 24 h. Other films of ReO_3 were deposited on the quartz windows of a small optical oven by heating the powders to temperatures greater than 200°C, while the windows was at room temperature.

Rhenium-oxide thin films were also deposited on glass substrates by reactive magnetron sputtering in a plasma-focusing dc magnetic field at a discharge power of 100 W. Metallic-rhenium (99.99%) plates were used as sputtering targets. A gas mixture of argon and oxygen was used as sputter atmosphere. The argon partial pressure was set at 0.040 Pa, with the oxygen partial pressure at 0.0067 Pa. The distance between the target and the substrate was 8 cm. The working pressure in a vacuum chamber during the sputtering process was 4 Pa.

Structural-phase analysis of the films was performed by XRD using PANalytical X'Pert PRO diffractometer, working in the Bragg-Brentano

θ–θ configuration. Conventional x-ray tube with Cu anode, operated at 45 kV and 40 mA, was used as an x-ray source. Raman spectra have been collected by a microprobe Jobin-Yvon Labram, equipped with a charge coupled device (CCD) detector. The low-frequency detection limit, due to the notch filter, was about 190 cm^{-1}. In all the experiments, a 50 $\times$ Mplan Olympus objective with numerical aperture of 0.70 was used. The power of the He-Ne laser (632.8 nm emission) out of the objective was about 5 mW, and the laser spot size was about 2–3 μm. To avoid unwanted laser-induced transformations, neutral filters of different optical densities (OD) were used, usually OD2 and OD1.

The asymmetric nematic liquid-crystalline cells were realized using a standard sandwich configuration, with one of the ITO electrodes covered by the rhenium-oxide thin film and the other electrode being a standard ITO-coated glass with a deposited layer of a rubbed polymer (polyimmide). The nematic liquid-crystalline layer (E7 by Merck) was confined between two transparent electrodes (thicknesses of liquid-crystalline layers were 8–36 μm).

Electro-optical response of the cells has been analyzed under the microscope with crossed polaroids equipped with a photodiode for light transmission measurement. Both broad-spectrum white-light illumination and red laser line (He-Ne 633 nm) were used. In all these measurements, the polyimmide-coated electrode was grounded, so that the phase of the electric voltages applied to the cell refers to the ReO_3 electrode.

RESULTS AND DISCUSSION

ReO_3 Powders

The high reactivity of the ReO_3 surface leads to an intercalation of foreign ions (protons) and to consequent structural modifications in an extended subsurface layer. The variations of such subsurface disorder are well reflected by the Raman spectra collected in samples having different histories of thermal treatments or exposure to the atmosphere. The perfect bulk structure does not generate Raman active modes because of its cubic symmetry, and the high electronic conductivity allows a penetration of the light for a depth of about 10–20 nm [8], so that all the observed Raman signal can be attributed to defect-induced scattering in subsurface region or to surface chemical species.

Representative examples of such variation are reported in Fig. 1. Spectrum A, was collected from a ReO_3 single crystal one day after heat treatment hotter than 200°C, which induced deintercalation of embedded hydrogen ions and a strong sublimation of the oxide layers

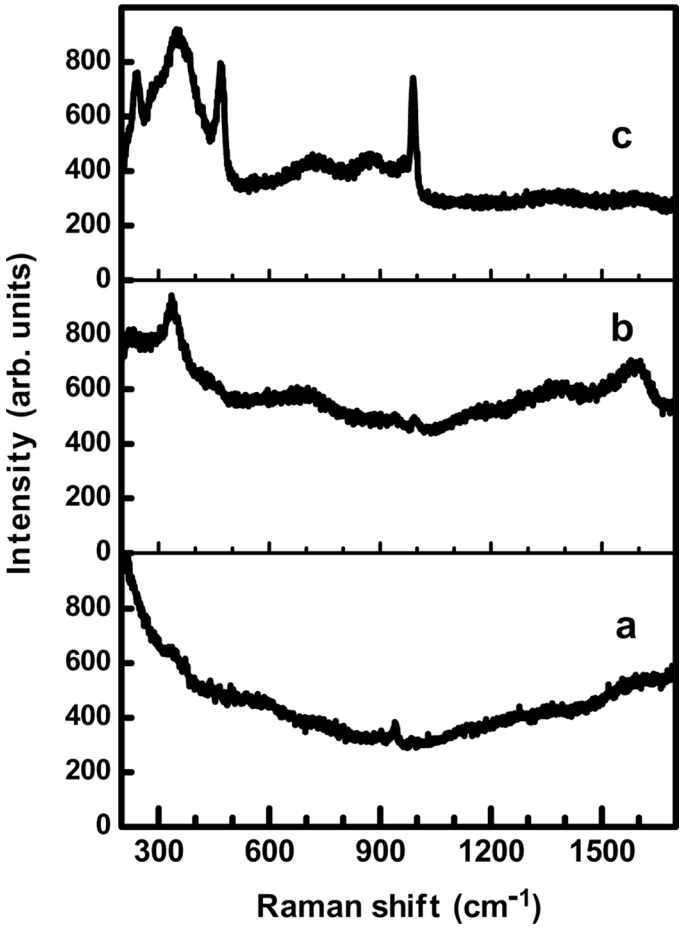

FIGURE 1 Raman spectra from different samples of ReO_3, collected with the same laser intensity and integration times: (a) single crystal one day after 200°C annealing; (b) commercial microcrystalline powders, after a long time of air exposure; (c) freshly smashed powders, after 10 min of grinding.

near the surface; this spectrum showed no evident spectral feature emerging from a low-frequency wing, except for a weak shoulder at about 330–340 cm^{-1}; it is close to the ideal spectrum expected for clean bulk rhenium oxide, where first-order Raman scattering is not allowed, and provides evidence of surface cleaning by sublimation. Spectrum B was collected from standard ReO_3 commercial powder, undergoing long-term exposure to air, from a sample zone corresponding to small microcrystal, and exhibits clearly a remarkable peak at about 335 cm^{-1}, which can be attributed to disorder in the surface

layers generated by long-term intercalation reactions with air moisture. Finally, spectrum C comes from smashed powder after 10 min of manual grinding. It is interesting to observe an appreciable rising up of the Raman peaks out of the background scattering in the standard powder with respect to the single crystal and a further enhancement of the Raman peaks after grinding, together with the rising up of new spectral features, besides the strongest sharp peak at $335\,cm^{-1}$: (i) new broad bands at about $720\,cm^{-1}$ and $870\,cm^{-1}$ and (ii) sharp peaks both at low (243, 345, $466\,cm^{-1}$) and high (960 and $988\,cm^{-1}$) frequencies, with an intensity increase correlated with the increasing milling times. The broad bands can be generated by the vibrational density of states of the octahedrally coordinated ReO_3 crystal off the Γ-point of the Brillouin zone, activated by the surface disorder [8]. The sharp peaks can be reasonably related to vibrations of surface molecular species, quickly formed at the most active sites of the freshly exposed ReO_3 surface; isolated or grouped ReO_4 could give rise to these observed peaks. Note that the typical spectrum of glassy carbon (D and G bands at about 1350 and $1580\,cm^{-1}$) was also found with variable intensity in the starting commercial powder (spectrum B), as a consequence of slow surface reaction with atmospheric CO_2. However, such a carbon signal appears quite lower in freshly smashed powder (spectrum C).

Films Deposited by Evaporation

The strong sublimation occurring at the surface of ReO_3 powder in air, when the temperature is greater than 200°C, can be exploited to obtain appreciable deposition of rhenium oxide on any substrate within a few centimetres from the heated powder. The resulting texture of the deposited films is shown in Figs. 2a and 2b, as it appears in optical microscope inspection. Most of the deposited thin films constitute a defective, hydrogen-containing phase, based on corner-sharing octahedra ReO_6, showing a red color (Fig. 2a). In fact, XRD patterns coming from such films (Fig. 3) are quite similar to those reported for powders purposely intercalated with hydrogen, whose composition is represented by the formula $H_{0.57}ReO_3$ [17].

Raman spectra collected from such films confirm the defective nature of the solid phase deposited by evaporation; the representative spectrum (a) in Fig. 4, collected in a region of Fig. 2a out of the scratch, is similar in shape to that of the rhenium-oxide powder shown in Fig. 1. However, the sharp Raman band at $340\,cm^{-1}$ and the broad one at about $720\,cm^{-1}$ exhibit a remarkable intensity enhancement, explained with a higher defect concentration than microcrystalline powder.

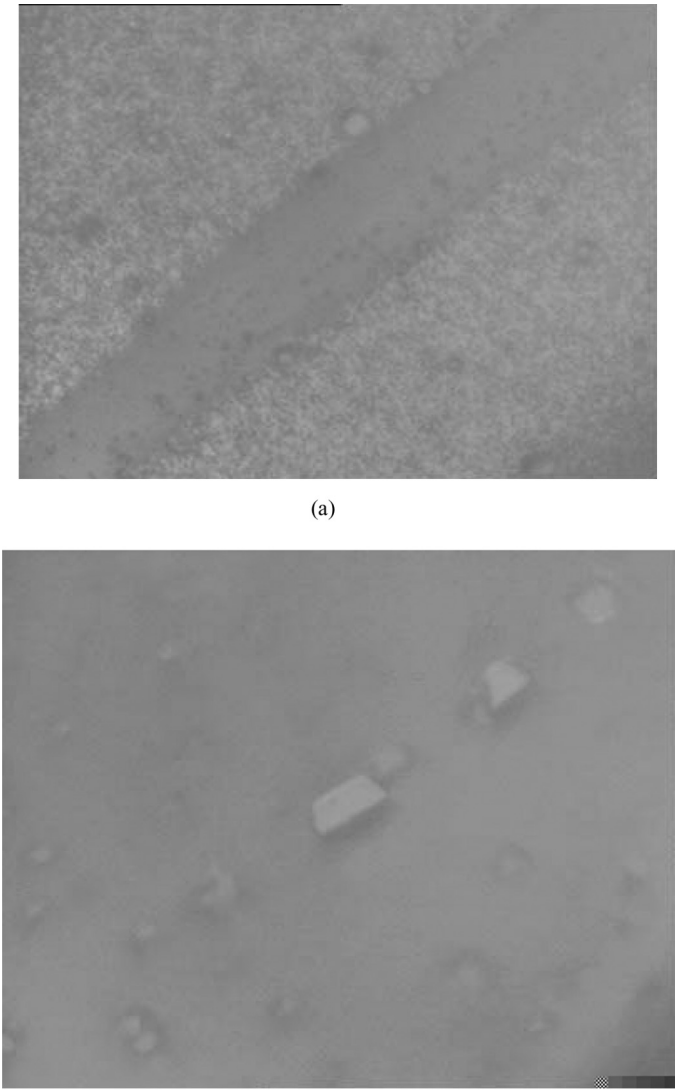

(a)

(b)

FIGURE 2 (a) Microscopic view of thermally evaporated film on glass from commercial powders heated at 210°C for about 24 h, zone of small red microcrystals, including a scratch that shows the color difference with respect to the substrate; (b) microscopic view of white trapezoidal single crystals, scattered in a rhenium-oxide film evaporated on glass.

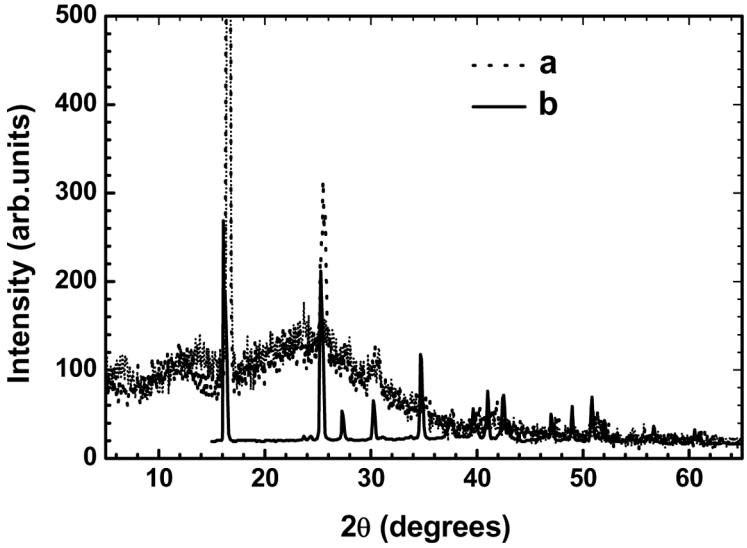

FIGURE 3 (a) XRD data of ReO_3 evaporated films, as described in the present work (dotted line); (b) XRD patterns, shown for comparison, from powders undergoing slow hydrogen intercalation and consequent structural change, reported from Ref. 17 (solid line).

Other different solid phases can be found in evaporated films, appearing as rectangular or trapezoidal crystals, giving a Raman spectrum with sharp peaks quite similar to those of $MReO_4$ perrhenates or ReO_4^- ion in solution [18,19]. In Fig. 2b, a micrographs of such a crystal is shown, and a typical Raman spectrum specific to that crystal is reported as spectrum (b) in Fig. 4. Some significant variation of the measured Raman frequency values among the different crystals observed in the deposited films can be explained with the occurrence of different phases based on perrhenate ions.

In general, spectra collected randomly from the deposited films indicate the presence of both octahedral and tetrahedral solid phases.

To study the properties of ReO_3 layers inserted in nematic liquid-crystalline cells, as well as for other potential applications, the deposition on ITO-coated glass substrates is necessary. It has been performed by exploiting the sublimation from of ReO_3 powders, as in the other depositions, but limiting the duration of the process to get very thin layers to preserve the optical transparency of the substrate. In fact, the Raman spectra collected from such deposited films show a small signal from rhenium oxide, superimposed on the strong background due to the substrate (Fig. 5).

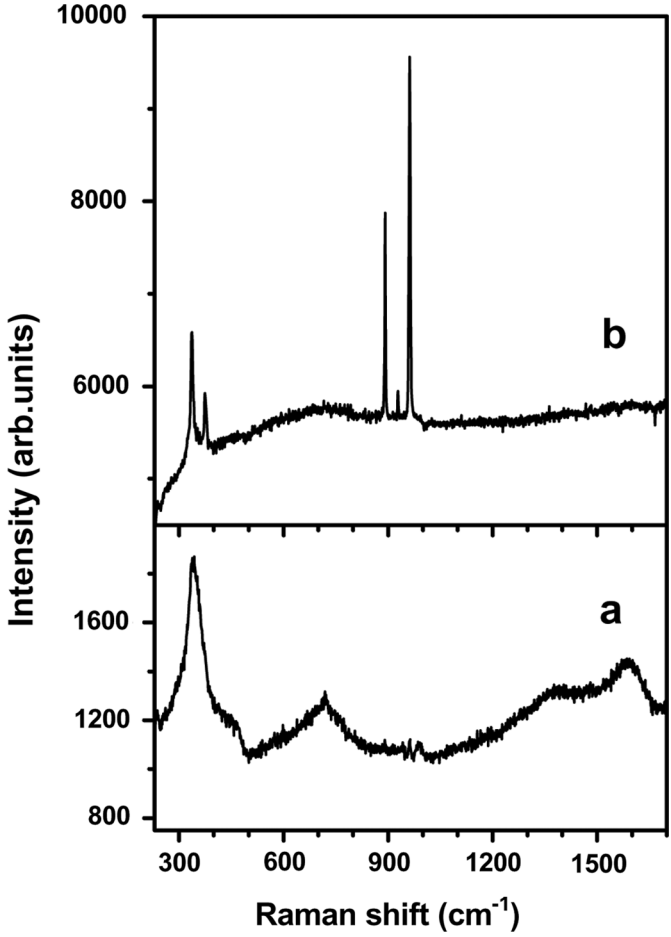

FIGURE 4 (a) Raman spectrum collected in air, at room temperature, from a deposited region of the film shown in Fig. 2a, below the scratch; (b) Raman spectrum collected selectively from the single crystal found in thermally evaporated films, shown in the center of Fig. 2b. Different acquisition conditions for (b) corresponds to a signal enhancement of a factor 1.5.

Sputtered Films

The deposition of thin films of ReO_3 has been performed also by using the technique of reactive magnetron sputtering. In Fig. 6, representative Raman spectra for films deposited by sputtering on pure glass substrate and on precoated Fe layers can be compared. As for thermally

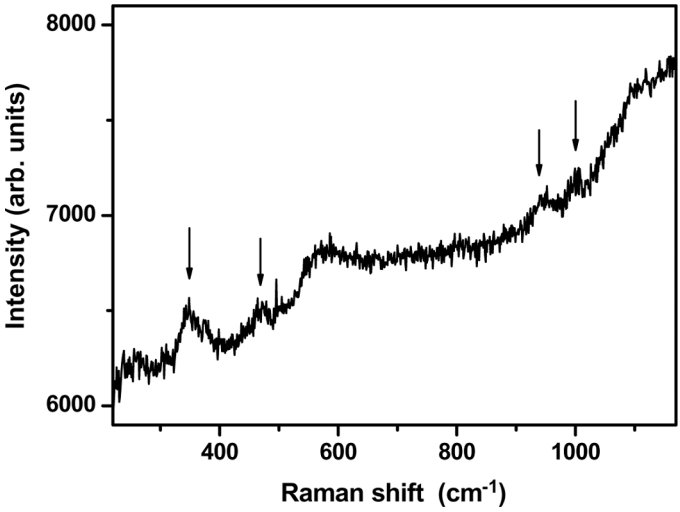

FIGURE 5 Raman spectrum from thin film of ReO_3 deposited on ITO-coated glass. The signal appears quite small with respect to the glass because of the small thickness. Arrows indicate the Raman bands associated with rhenium oxide.

evaporated films, two types of solid phases are also observed. Many distinct crystals have a crystal structure based on ReO_4 tetrahedral groups, generating the typical Raman spectrum of narrow strong peaks (spectrum A), whereas most of the film shows a spectrum of a disordered, defective solid phase, based on corner-sharing ReO_6 octahedra (spectrum B).

Protonic Conductivity of Evaporated Films

ReO_3 films have been deposited by evaporation on ITO-coated glasses, to be used as an electrode in asymmetric Nematic Liquid Crystal (NLC) cells. Preliminary impedance measurements have been performed on the films to check if the conductivity values are comparable with other proton-containing oxide films, which have been successfully tested in NLC cells.

In Figs. 7a and 7b, the frequency dispersion curves of the real and imaginary parts of the film impedance are reported. The interesting information is the value of the cutoff frequency, which is found in the range 10^4–10^5 Hz, consistent with the hypothesis of proton conductivity and well comparable with the values found in similar films of oxide doped with some amount of protons [11].

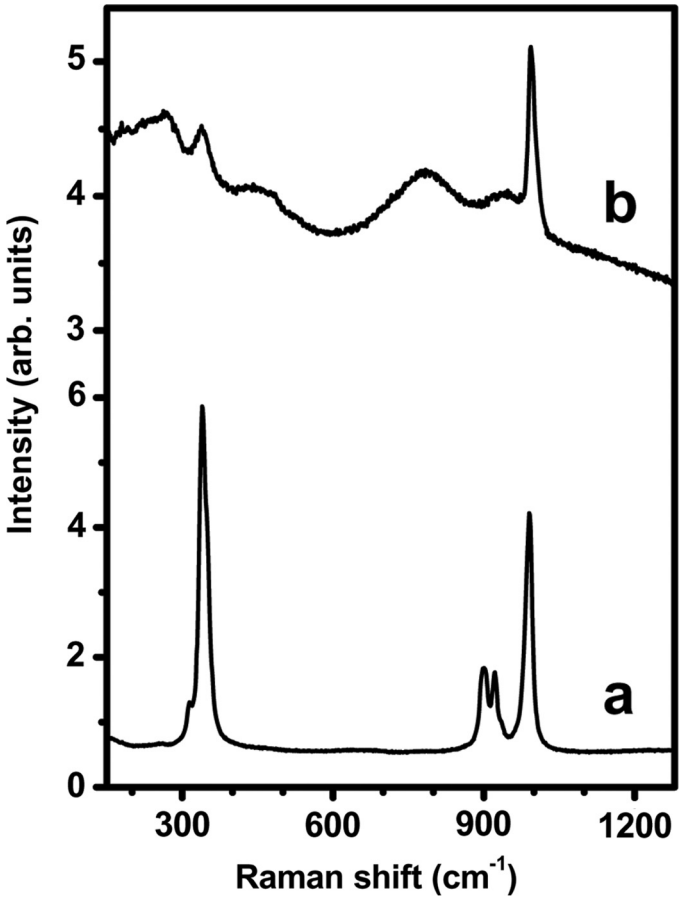

FIGURE 6 Raman spectra from the sputtered film. The spectrum (a) coming only from the single crystals, with sharp peaks, is compared with the spectrum (b) collected in the region between the crystals. In both cases, the measurements have been performed in conditions to get strong signal, at expense of spectral resolution (wide slits). The intensity units have been divided by a factor of 10^4 to make the graph more readable.

Application to Liquid-Crystalline Cells

After the discovery of the rectifying effect of tungsten trioxide in asymmetric NLC cell [10], several investigations [11–16] have been carried out on various metal oxides containing some amount of mobile protons. Therefore, it is interesting to test the response of rhenium oxide coated electrodes, after the evidence of a sufficient ionic

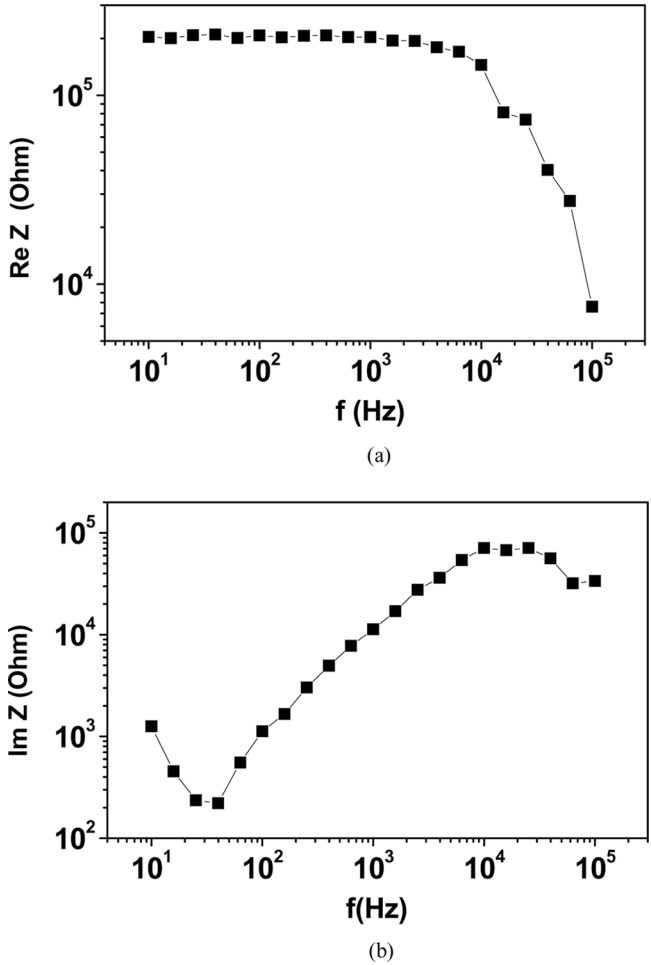

FIGURE 7 (a) Real part of complex impedance of evaporated ReO_3 film vs. frequency of applied voltage, (b) same plot vs. frequency for the imaginary part of the impedance.

conductivity, due to the proton content of the solid phases of the films. As in the case of tungsten oxide, the application of a low-frequency electric field (square wave shaped) perpendicular to the liquid crystal–electrode interface induces an asymmetric optical switching, as can be seen in the plot of electro-optical response shown in Fig. 8. In these experiments, the light transmitted by the sample in a crossed-polarizer configuration was measured by a photodiode detector. The asymmetric response does not depend on the thickness of

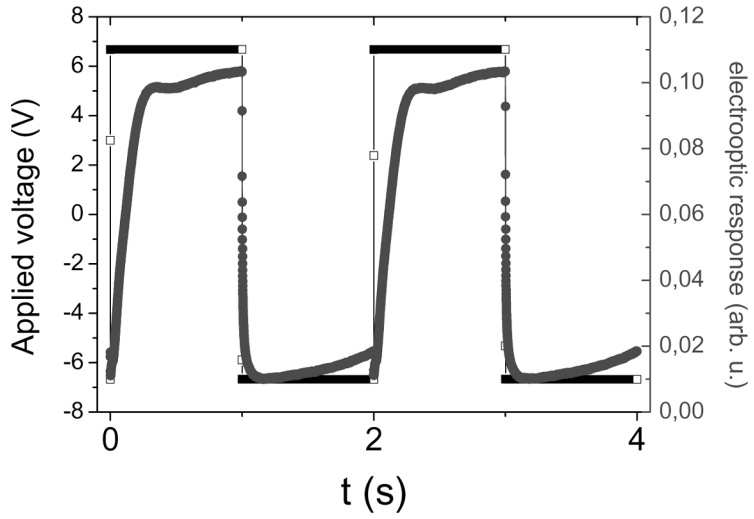

FIGURE 8 Electro-optic response of an asymmetric NLC cell containing a thin film of ReO_3 deposited on one of the two ITO electrodes. The amount of transmitted light through a crossed polaroids microscope, measured by a photodiode, is plotted versus time, together with the applied external voltage, square-wave shaped, always with reference to the electrode coated with rhenium oxide.

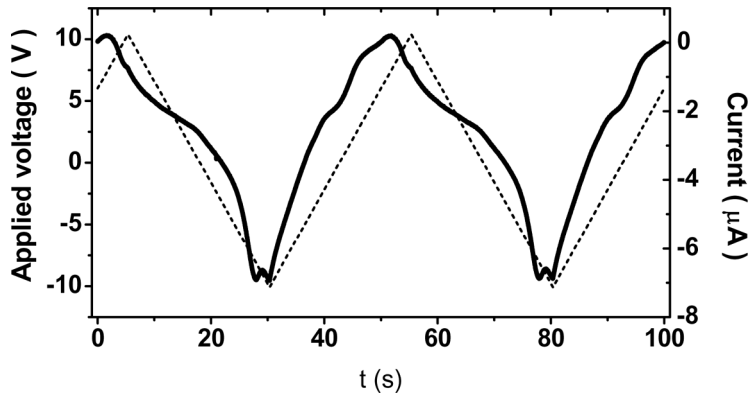

FIGURE 9 Plot of the current flowing across the entire NLC asymmetric cell, when an external voltage is applied, with a triangular wave shape. The voltage is measured on the ReO_3-coated electrode, while the other one is grounded.

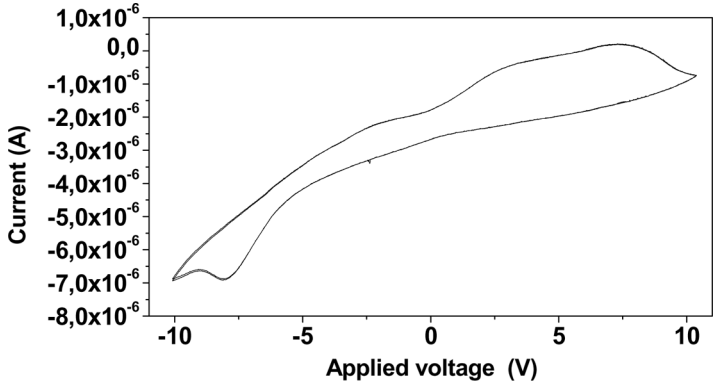

FIGURE 10 Cyclic voltammetry curve of the asymmetric NLC cell containing the ReO_3 electrode, obtained from triangular-shaped wave.

the liquid-crystalline layers, whereas it depends on the amplitude and frequency of the perturbing electric field.

Electric-characterization measurements have been performed on the cell to investigate the possible electrochemical phenomena associated with the presence of the mixed conductor ReO_3.

The current response, of the order of μA, can be measured for the entire cell when an external voltage, up to about 10 V, is applied. In Fig. 9, the triangular wave of the applied voltage and the current response are shown together. A cyclic voltammetry plot (Fig. 10), obtained from such kind of measurement, shows clearly a non-ohmic behavior.

It is worth remarking that such a voltammogram is similar to that provided by the WO_3 films inserted in the cell. This last evidence seems to support an explanation of the unusual switching response of the cell as due to a reverse internal electric field generated by the particular distribution of mobile ions at the interfaces. It could be associated with a deintercalation of small ions, coming from the rhenium-trioxide layer and migrating toward the NLC Layer during the anodic phase.

CONCLUSIONS

Commercial ReO_3 powder was used to obtain thin films with different solid phases and containing an appreciable amount of hydrogen ions. Although more careful structural investigations are needed to know the crystallographic details of such solid phases, two types have to be considered: (i) $HxReO_3$ compounds with corner-sharing octahedral ReO_6 units, more or less distorted by the hydrogen intercalation, with red color, metal-like electronic conductivity, and high surface

reactivity toward water and CO_2; (ii) $HReO_4$-based crystals, transparent, insulating, and not very reactive with atmospheric gases. The actual films contain these two components in different amounts and with different texture. The films have shown evidence of a sufficient combination of electronic and ionic conductivities to give good results as rectifying layers in NLC cells, compared to films of tungsten trioxide, well known for its electrochromic applications.

ACKNOWLEDGMENTS

The authors are indebted to Tiziana Barone and Giuseppe De Santo for their help in the evaporation of ReO_3 films and the sequential Raman measurements. A. Kuzmin thanks the University of Trento and the CeFSA laboratory of ITC-CNR (Trento) for hospitality and financial support. This research was partly supported by the Latvian Government Research Grant Nos. 05.1714 and 05.1717.

REFERENCES

[1] Allen, P. B. & Schulz, W. W. (1993). *Phys. Rev. B*, *47*, 14434.
[2] Pearsall, T. P. & Lee, C. A. (1974). *Phys. Rev. B*, *10*, 2190.
[3] King, C. N., Kirsch, H. C., & Geballe, T. H. (1971). *Solid State Commun.*, *9*, 907.
[4] Tanaka, T., Akahane, T., Bannai, E., Kawai, S., Tsuda, N., & Ishizawa, Y. (1976). *J. Phys. C: Solid State Phys.*, *9*, 1235.
[5] Jorgensen, J.-E., Jorgensen, J. D., Batlogg, B., Remeika, J. P., & Axe, J. D. (1986). *Phys. Rev. B*, *33*, 4793.
[6] Chang, T. S. & Trucano, P. (1978). *J. Appl. Cryst.*, *11*, 286.
[7] Goodenough, J. B. (1971). *Prog. Solid State Chem.*, *5*, 145.
[8] Purans, J., Kuzmin, A., Cazzanelli, E., & Mariotto, G. (2007). *J. Phys.: Condens. Matter*, *19*, 26206.
[9] Horiuchi, S., Kimizuca, N., & Yamamoto, A. (1979). *Nature*, *279*, 226.
[10] Strangi, G., Lucchetta, D. E., Cazzanelli, E., Scaramuzza, N., Versace, C., & Bartolino, R. (1999). *Appl. Phys. Lett.*, *4*, 534.
[11] Bruno, V., Cazzanelli, E., Scaramuzza, N., Strangi, G., Ceccato, R., & Carturan, G. (2002). *J. Appl. Phys.*, *92*, 5340.
[12] Cazzanelli, E., Marino, S., Bruno, V., Castriota, M., Scaramuzza, N., Strangi, G., Versace, C., Ceccato, R., & Carturan, G. (2003). *Solid State Ionics*, *165*, 201.
[13] Marino, S., Castriota, M., Bruno, V., Cazzanelli, E., Strangi, G., Versace, C., & Scaramuzza, N. (2005). *J. Appl. Phys.*, *97*, 013523.
[14] Castriota, M., Marino, S., Versace, C., Strangi, G., Scaramuzza, N., & Cazzanelli, E. (2005). *Mol. Cryst. Liquid Cryst.*, *429*, 237.
[15] Marino, S., Castriota, M., Strangi, G., Cazzanelli, E., & Scaramuzza, N. (2007). *J. Appl. Phys.*, *102*, 013112-1.
[16] Bruno, V., Castriota, M., Marino, S., Versace, C., Strangi, G., Cazzanelli, E., & Scaramuzza, N. (2005). *Mol. Cryst. Liquid Cryst.*, *441*, 27.
[17] Majid, C. A. & Hussain, M. A. (1995). *J. Phys. Chem. Solids*, *56*, 255.
[18] Beattie, I. R. & Ozin, G. A. (1969). *J. Chem. Soc. A*, *2615*.
[19] Hard, F. D., Wachs, I. E., Horsley, J. A., Via, G. H. (1988). *J. Mol. Cat.*, *46*, 15.